

Ra excesses measured in MORB to date<sup>8</sup> all come from a graben in the Siqueiros Transform, which has undergone relatively recent extension.

The effect of variable viscosity and density on melt segregation beneath mid-ocean ridges is shown schematically in Fig. 3. A small amount of volatile-rich melt is formed in the upwelling part of the mantle as decarbonation reactions or by oxidation if carbon is stored as graphite or diamond. As water is incompatible in nominally anhydrous minerals relative to melt, it will partition into the melt, although the release might be gradual<sup>32</sup>. This volatile-rich melt is able to move at small porosities because of its low viscosity and density. Because the contribution of this melt to the volume of erupted basalts is small, its incompatible element-enriched character is lost, but isotopic disequilibria are not affected by dilution. Owing to incomplete extraction, some melt (more than 1%) remains in a broad zone, consistent with the observations from the MELT experiment. A two-stage melting model could also explain the depleted character of clinopyroxene in abyssal peridotites<sup>1</sup>. Modelling<sup>28</sup> showed that the observed rare earth element patterns require low porosities only at one stage but not throughout melt extraction. □

Received 15 September 2000; accepted 12 February 2001.

1. Johnson, K. H., Dick, H. J. B. & Shimizu, N. Melting in the oceanic upper mantle: An ion microprobe study of diopsides in abyssal peridotites. *J. Geophys. Res.* **95**, 2661–2678 (1990).
2. Spiegelman, M. & Elliott, T. Consequences of melt transport for uranium series disequilibrium in young lavas. *Earth Planet. Sci. Lett.* **118**, 1–20 (1993).
3. Richardson, C. & McKenzie, D. Radioactive disequilibria from 2D models of melt generation by plumes and ridges. *Earth Planet. Sci. Lett.* **128**, 425–437 (1994).
4. Lundstrom, C. C., Gill, J., Williams, Q. & Perfit, M. R. Mantle melting and basalt extraction by equilibrium porous flow. *Science* **270**, 1958–1961 (1995).
5. Salters, V. J. M. & Longhi, J. Trace element partitioning during the initial stages of melting beneath mid-ocean ridges. *Earth Planet. Sci. Lett.* **166**, 15–30 (1999).
6. Lundstrom, C. C., Williams, Q. & Gill, J. B. Investigating solid mantle upwelling rates beneath mid-ocean ridges using U-series disequilibria, 1: a global approach. *Earth Planet. Sci. Lett.* **157**, 151–165 (1998).
7. Lundstrom, C. C., Gill, J. & Williams, Q. A geochemically consistent hypothesis for MORB generation. *Chem. Geol.* **162**, 105–126 (2000).
8. Lundstrom, C. C., Sampson, D. E., Perfit, M. R., Gill, J. & Williams, Q. Insights into mid-ocean ridge basalt petrogenesis: U-series disequilibria from the Siqueiros Transform, Lamont Seamounts, and East Pacific Rise. *J. Geophys. Res.* **104**, 13035–13048 (1999).
9. The MELT Seismic Team. Imaging the deep seismic structure beneath a mid-ocean ridge: the MELT experiment. *Science* **280**, 1215–1218 (1998).
10. Faul, U. H., Toomey, D. R. & Waff, H. S. Intergranular basaltic melt is distributed in thin, elongated inclusions. *Geophys. Res. Lett.* **21**, 29–32 (1994).
11. Turcotte, D. L. & Schubert, G. *Geodynamics* (John Wiley, New York, 1982).
12. von Bargen, N. & Waff, H. S. Permeabilities, interfacial areas and curvatures of partially molten systems: Results of numerical computations of equilibrium microstructures. *J. Geophys. Res.* **91**, 9261–9276 (1986).
13. Zhu, W., David, C. & Wong, T.-f. Network modeling of permeability evolution during cementation and hot isostatic pressing. *J. Geophys. Res.* **100**, 15451–15464 (1995).
14. Wark, D. A. & Watson, E. B. Grain-scale permeabilities of texturally equilibrated, monomineralic rocks. *Earth Planet. Sci. Lett.* **164**, 591–605 (1998).
15. Faul, U. H. Permeability of partially molten upper mantle rocks from experiments and percolation theory. *J. Geophys. Res.* **102**, 10299–10311 (1997).
16. Bourbie, T. & Zinsner, B. Hydraulic and acoustic properties as a function of porosity in Fontainebleau sandstone. *J. Geophys. Res.* **90**, 11524–11532 (1985).
17. McKenzie, D. Some remarks on the movement of small melt fractions in the mantle. *Earth Planet. Sci. Lett.* **95**, 53–72 (1989).
18. Spiegelman, M. UserCalc: A Web-based uranium series calculator for magma migration problems. *Geochem. Geophys. Geosyst.* **1**, 1999 GC 0000 30 (2000).
19. Michael, P. Regionally distinctive sources of depleted MORB: Evidence from trace elements and H<sub>2</sub>O. *Earth Planet. Sci. Lett.* **131**, 301–320 (1995).
20. Zhang, Y. & Zindler, A. Distribution and evolution of carbon and nitrogen in the Earth. *Earth Planet. Sci. Lett.* **117**, 331–345 (1993).
21. Green, D. H. & Liebermann, R. C. Phase equilibria and elastic properties of a pyrolite model for the oceanic upper mantle. *Tectonophysics* **32**, 61–92 (1976).
22. Blundy, J. D., Brodholt, J. P. & Wood, B. J. Carbon-fluid equilibria and the oxidation state of the upper mantle. *Nature* **349**, 321–324 (1991).
23. Mibe, K., Fujii, T. & Yasuda, A. Connectivity of aqueous fluid in the Earth's upper mantle. *Geophys. Res. Lett.* **25**, 1233–1236 (1998).
24. Dobson, D. P. et al. In-situ measurement of viscosity and density of carbonate melts at high pressure. *Earth Planet. Sci. Lett.* **143**, 207–215 (1996).
25. Hunter, R. H. & McKenzie, D. The equilibrium geometry of carbonate melts in rocks of mantle composition. *Earth Planet. Sci. Lett.* **92**, 347–356 (1989).
26. Galer, S. J. G. & O'Nions, R. K. Magmagenesis and the mapping of chemical and isotopic variations in the mantle. *Chem. Geol.* **56**, 45–61 (1985).
27. Plank, T. & Langmuir, C. H. Effects of the melting regime on the composition of the oceanic crust. *J. Geophys. Res.* **97**, 19749–19770 (1992).

28. Kelemen, P. B., Hirth, G., Shimizu, N., Spiegelman, M. & Dick, H. J. B. A review of melt migration processes in the adiabatically upwelling mantle beneath oceanic spreading ridges. *Phil. Trans. R. Soc. Lond. A* **355**, 283–318 (1997).
29. Yaxley, G. M. Experimental study of the phase and melting relations of homogeneous basalt + peridotite mixtures and implications for the petrogenesis of flood basalts. *Contrib. Mineral. Petrol.* **139**, 326–338 (2000).
30. Asimow, P. D. & Stolper, E. M. Steady-state mantle–melt interactions in one dimension: I. Equilibrium transport and melt focusing. *J. Petrol.* **40**, 475–494 (1999).
31. Nielsen, R. L., Sours-Page, R. E. & Harpp, K. S. Role of a Cl-bearing flux in the origin of depleted ocean floor magmas. *Geochem. Geophys. Geosyst.* **1**, 1999 GC 0000 17 (2000).
32. Hirth, G. & Kohlstedt, D. L. Water in the oceanic upper mantle: implications for rheology, melt extraction and evolution of the lithosphere. *Earth Planet. Sci. Lett.* **144**, 93–108 (1996).
33. Wood, B. J., Blundy, J. D. & Robinson, J. A. C. The role of clinopyroxene in generating U-series disequilibrium during mantle melting. *Geochim. Cosmochim. Acta* **63**, 1613–1620 (1999).

**Acknowledgements**

Discussions with S. Eggins, D. Green and H. O'Neill are gratefully acknowledged, as well as pre-publication access to a G<sup>3</sup> article by M. Spiegelman. Reviews by T. Elliot and M. Spiegelman helped to shape this manuscript.

Correspondence and requests for materials should be addressed to the author (e-mail: uli.faul@anu.edu.au).

.....  
**Towards a general theory of biodiversity**

**Elizaveta Pachepsky\*†, John W. Crawford†, James L. Bown† & Geoff Squire\***

† SIMBIOS Centre, School of Computing, University of Abertay Dundee, Dundee DD1 1HG, UK

\* Vegetation Systems Unit, Scottish Crop Research Institute, Invergowrie, Dundee DD2 5DA, UK

.....  
 The study of patterns in living diversity is driven by the desire to find the universal rules that underlie the organization of ecosystems<sup>1,2</sup>. The relative abundance distribution, which characterizes the total number and abundance of species in a community, is arguably the most fundamental measure in ecology. Considerable effort has been expended in striving for a general theory that can explain the form of the distribution<sup>3,4</sup>. Despite this, a mechanistic understanding of the form in terms of physiological and environmental parameters remains elusive<sup>5</sup>. Recently, it has been proposed that space plays a central role in generating the patterns of diversity<sup>6,7</sup>. Here we show that an understanding of the observed form of the relative abundance distribution requires a consideration of how individuals pack in time. We present a framework for studying the dynamics of communities which generalizes the prevailing species-based approach to one based on individuals that are characterized by their physiological traits. The observed form of the abundance distribution and its dependence on richness and disturbance are reproduced, and can be understood in terms of the trade-off between time to reproduction and fecundity.

The relative abundance distribution describes how the individuals in a community are partitioned among rare and common species. A log-normal form of the distribution, implying a community containing many rare species and relatively few common ones, is associated with a community in equilibrium. A power-law (or geometric) form, implying a more equitable share of individuals amongst species groups, is associated with non-equilibrium behaviour resulting from perturbation due to disturbance, pollution or immigration<sup>8</sup>. Two pervasive theories—multiplicative recruitment<sup>3</sup> and sequential niche breakage<sup>4</sup>—attempt to explain the emergent log-normal form of the abundance distribution in general terms, but neither of these provides an explanation of the observed

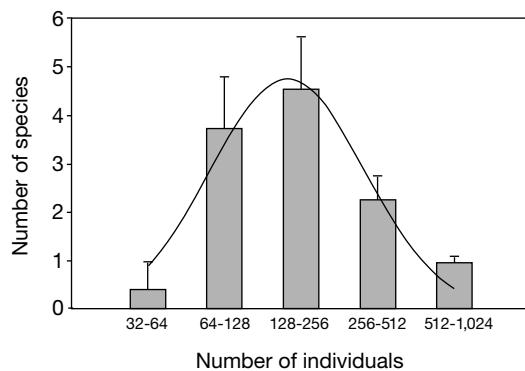


**Figure 1** Sample abundance distribution on a  $30 \times 30$  lattice. The histogram values were averaged over the time of coexistence of 15 plant types, and the error bars (corresponding

to the standard deviation) give an indication of the variation in time within the abundance classes.

patterns<sup>5</sup>. An explanation in terms of immigration, migration and speciation at the metapopulation scale has been developed<sup>9</sup>, but is phenomenological and does not address the origins of relative abundance at the population scale. Fundamentally, few models employ parameters that can be measured directly in individuals, and almost all average out the substantial variation that exists between individuals of the same species. Therefore, the functional properties of individuals and the resulting state of the community cannot be mechanistically linked, and this fuels the topical debate on the relation between biological diversity and community function<sup>10</sup>.

To address these issues, we have developed an individual-based model with three main features. (1) Individual-based—a plant community is modelled by explicitly simulating development of each individual plant in terms of physiological traits. The spread of values of the plants' traits forms a probability distribution of trait values that defines the diversity in a community. This departs from the usual definition of diversity based on species, and leads to a definition in terms of the variables governing the dynamics of the community. (2) Spatially explicit—individuals are located at nodes on a discrete spatial lattice, and interact within a neighbourhood that depends on each plant's development stage. Only one plant can exist at each lattice location. Nutrients are depleted from the resource base in accordance with plants' uptake. The resource base is distributed uniformly in space, because the focus of the work reported here is on the role of individual behaviour in promoting diversity. (The effect of environmental heterogeneity on diversity is well documented<sup>6,11</sup>.) We assume that the lattice represents an isolated community<sup>6</sup>; that is, we exclude the effects of immigration, and seeds that land outside the lattice do not contribute to the dynamics. (3) Process-based—a crucial feature of the approach is that the traits represent physiological processes characterized by experimentally derived parameters. An individual is defined in terms of 12 traits that relate to resource uptake, area over which resource is captured, internal allocation of resources between structure, storage and reproduction, time of reproduction, number of progeny produced, dispersal of progeny, and survival. Traits are primarily functions of a plant's development state. Competition in the model occurs for resource and for space. The resource competition occurs when more than one plant takes up resource from the same location on the lattice, in which case the resource is distributed in proportion to plants' current resource uptake. Competition for space occurs when seeds are distributed on the lattice. A seed germinates only if it falls on an empty lattice location. In the results reported here, dispersal area is constant for all plants, and the seeds are dispersed randomly. An analysis of the effect of varying the dispersal parameters showed that diversity increases as dispersal is progressively reduced below the level of complete mixing, and was consistent with the results of previous studies<sup>7,12–14</sup>. To eliminate

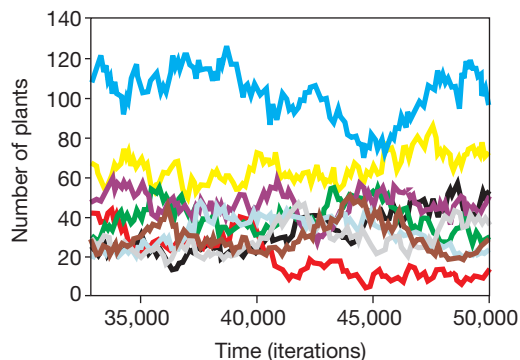


**Figure 2** Evolution of abundance of nine plant types in time on a  $20 \times 20$  lattice.

geneflow as a cause of any observed pattern, individuals reproduce clonally in this study. The full set of parameters and the corresponding probability density functions were derived from experiments conducted on the grassland species *Rumex acetosa* L. as part of a wider study of the dynamics of species-rich grasslands (U. Bausenwein *et al.*, manuscript in preparation).

The model was initialized with 75 plants randomly located on the lattice, and with trait value sets randomly selected from the trait probability density functions. The size of the lattices used range from  $10 \times 10$  to  $50 \times 50$  (equivalent to approximately  $1 \text{ m}^2$  to  $25 \text{ m}^2$  for *R. acetosa*). The model was run for 50,000 iterations, corresponding to approximately 1,250 generations. In the initial stages, the number of types decreased exponentially with time, such that only half the number of types remained after an average of 5,000 iterations. Subsequently, a dynamic equilibrium was achieved with the number of types remaining constant for at least 1,000 generations. The number of coexisting types depended on the area of the lattice. Across the range of scales studied, the dependence on area was of a power-law form with exponent equal to  $0.4 \pm 0.06$ , consistent with the range observed in real ecological communities<sup>15</sup>.

The resulting abundance distribution was of log-normal form for the cases where the system had been in equilibrium for the longest time, and where a sufficiently large number of individuals remained at the end of the exponential phase for meaningful statistics ( $P > 0.2$  for the Kolmogorov–Smirnov test with Lilliefors corrected critical values<sup>16</sup>). An example is shown in Fig. 1. During the exponential phase, the abundance distribution was more similar to the geometric form observed for disturbed or non-equilibrium communities. Not only is the log-normal form of the species relative abundance distribution reproduced, but the correspondence between the standard deviation of the

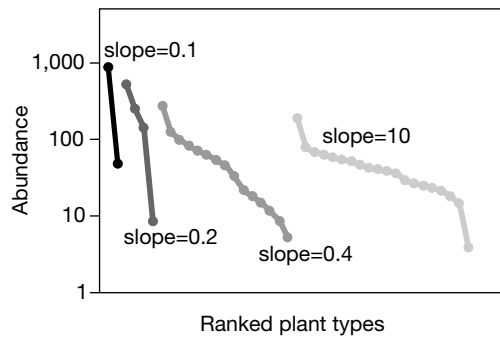


**Figure 3** Effect of the trade-off between time of reproduction and fecundity on the shape of the abundance curve on a  $50 \times 50$  lattice. Results were obtained from a simplified version of the individual-based model with fecundity = slope  $\times$  (time of reproduction) + 1.5. Individual mortality is random, with a probability of 0.001 per cycle.

distribution and richness (that is, the total number of types) is the same as that observed in communities of less than a few hundred species<sup>4</sup>. The parameters are also stable over time, despite the fact that the ranks of plant types are not constant. In all cases, there was clear stratification in the abundance classes (Fig. 2). In particular, we observed that the most abundant individuals in the community also had the most stable numbers. The ranks within the least abundant classes appeared to be governed by stochastic processes relating to competition for the space vacated through death of a resident. This dynamic behaviour of abundance has been observed in communities of ground beetles<sup>17</sup> and plankton<sup>18</sup>, and illustrates the underlying dynamic form of the equilibrium state. Although the trait values of the modelled population are based on ranges observed in a particular species, *R. acetosa*, the model produces general patterns that are common to various ecological communities.

In order to identify the aspects of individual variation that were required to generate the observed diversity patterns, the effect of the variation of each of the physiological traits was studied. This was done by replacing the probability distribution by the mean value for each trait in turn, and looking at the effect on the diversity in the simulated communities. Of the 12 traits in the model, only variation in those affecting time to reproduction and fecundity was found to influence the abundance of individuals in the community. A plot of time to reproduction against fecundity for the coexisting individuals revealed an approximately linear trade-off. This observation allowed us to reduce the complexity of the model from a form using 12 traits to one using only three: time of reproduction, a linear relation (trade-off) between time of reproduction and fecundity, and a small random death factor (see Fig. 3). In the simplified model, a lattice is populated by individuals that vary in their time to reproduction and produce an amount of seed in accordance with the trade-off, disperse this seed as in the full model, and die at random. The initial conditions, the lattice size and the duration of the simulation were as described above. This model exhibited the same underlying dynamics, abundance distribution and species-area curve to that observed in the full model. Furthermore, simulations showed that the parameters of the predicted abundance distribution were sensitive to the form of the trade-off (Fig. 3). The important environmental factor in the model was weak stochastic disturbance in the form of random death of a small percentage of individuals. Without this, richness was significantly reduced.

The generality of these conclusions can be established using a mathematical model that incorporates the basic processes governing the dynamics of most ecological communities: competition for resource, reproduction and death. The local interactions between individuals are ignored in this model, and individuals are assumed

Box 1

Three-dimensional trait-space model

In the mean-field model, we assume that four processes define an individual in terms of its contribution to the dynamics of the community: birth, competition, reproduction and death. Thus an individual is characterized by the time to reproduction,  $1/\lambda$ ; lifetime,  $1/a$ ; the number of progeny produced per unit time,  $b$ ; and the competition that arises through density-dependent interactions between individuals. The model describes the effect of competition on the rate of conversion of non-reproductive juveniles,  $s_{\lambda,a,b}$ , into reproductive adults,  $f_{\lambda,a,b}$ . The diversity of the community is described by the frequency distribution of  $f_{\lambda,a,b}$  and  $s_{\lambda,a,b}$  across the trait values:

$$\frac{\partial f_{\lambda,a,b}(t)}{\partial t} = \frac{\lambda s_{\lambda,a,b}(t)}{1 + K \int_0^{\lambda_c} \kappa(x - \lambda) s_{x,a,b}(t) dx} - a f_{\lambda,a,b}(t)$$

$$\frac{\partial s_{\lambda,a,b}(t)}{\partial t} = b \int_{\Omega_x} \int_{\Omega_y} p(\mathbf{u}|\mathbf{x}, \mathbf{y}) G[f_x, f_y] dx dy - c \lambda s_{\lambda,a,b}(t)$$

The single integral term arises from the assumption that competition between individuals depends on their relative times to reproduction through the form of  $\kappa$ . Both  $K$  and  $c$  are assumed constant, and  $1/\lambda_c$  is the minimum time to reproduction. Geneflow is expressed through the function  $p(\mathbf{u}|\mathbf{x}, \mathbf{y})$  that describes the probability that an individual of type  $\mathbf{u} = \{\lambda, a, b\}$  results from a cross between individuals of types  $\mathbf{x} = \{\lambda_x, a_x, b_x\}$  and  $\mathbf{y} = \{\lambda_y, a_y, b_y\}$ , which are two points in the three-dimensional space of the parameters  $\lambda$ ,  $a$  and  $b$ . The function  $G[f_x, f_y]$  describes the frequency of crossing between individuals of type  $\mathbf{x}$  and  $\mathbf{y}$ , and the integral is over the parameter space,  $\Omega_x$  and  $\Omega_y$ .

The analytical solutions of this model quoted in the text refer to the case where we have assumed for simplicity that  $\kappa$  can be approximated by the Heaviside function,  $u_\lambda(x)$  (that is,  $u_\lambda(x) = 0$  for  $x < \lambda$  and  $u_\lambda(x) = 1$  for  $x \geq \lambda$ ). The special case of clonal reproduction is accommodated by replacing the double integral term by the term  $b f_{\lambda,a,b}(t)$ . Therefore, we consider solutions to the system:

$$\frac{\partial f_{\lambda,a,b}(t)}{\partial t} = \frac{\lambda s_{\lambda,a,b}(t)}{1 + K \int_0^{\lambda_c} s_{x,a,b}(t) dx} - a f_{\lambda,a,b}(t)$$

$$\frac{\partial s_{\lambda,a,b}(t)}{\partial t} = b f_{\lambda,a,b}(t) - c \lambda s_{\lambda,a,b}(t)$$

The steady-state solutions of this system require that  $b/a$  is a function of  $\lambda$ , otherwise the distribution along  $\lambda$  collapses to a point at  $\lambda_c$ . The steady-state solutions are

$$s_{\lambda,a,b}(t) = - \frac{1}{cK} \frac{d}{d\lambda} \left( \frac{b(\lambda)}{a(\lambda)} \right) \tag{1}$$

$$f_{\lambda,a,b}(t) = - \frac{\lambda}{Kb(\lambda)} \frac{d}{d\lambda} \left( \frac{b(\lambda)}{a(\lambda)} \right) \tag{2}$$

with an additional condition that  $b(1)/a(1) = 1$ .

From (1) it follows that  $d[b(\lambda)/a(\lambda)]/d\lambda < 0$ , that is,  $b(\lambda)/a(\lambda)$  must be monotonic decreasing. Moreover, the linear stability analysis shows that for non-zero steady state, it is necessary that  $d^2[b(\lambda)/a(\lambda)]/d\lambda^2 > 0$ , that is, that  $b(\lambda)/a(\lambda)$  is concave up. The non-zero steady state is stable if  $b(\lambda)/a(\lambda) > cK$ , and otherwise the 0-state is stable.

Using heuristic forms for  $\mathbf{p}$  and  $\mathbf{G}$ , it can be shown that the effect of trade-offs on the abundance curve can be modified by geneflow through the form of the dependence of the product of  $\mathbf{p}$  and  $\mathbf{G}$  on the parameters.

to be spatially well mixed. The dynamics of the community can then be described by two ordinary differential equations (Box 1) describing the time evolution of the system in a three-dimensional trait space. The traits that characterize the above processes are the time to reproduction ( $1/\lambda$ ), the characteristic lifespan ( $1/a$ ), and fecundity ( $b$ ). The solution shows that unless the ratio  $b/a$  is a function of  $\lambda$ , the system collapses to a state where only the fastest

reproducing individuals remain. Therefore, an interdependence between time to reproduction and at least one of longevity or fecundity is required to maintain diversity. The form of the trade-off determines the shape of the distribution of abundance of coexisting individuals across the trait space and the stability of that distribution (Box 1).

These results confirm the main features of the individual-based model—that the trade-off between time to reproduction and fecundity sustains the diversity in the community, and governs the form of the resulting abundance distribution. The trade-off is a simple but fundamental example of the link between individual- and community-scale features of the system. Its central role suggests that an explanation of community dynamics must incorporate an account of individual behaviour. Furthermore, by integrating more complex mechanisms encompassing uptake, competition and the effect of the nutritional status of an individual on its fecundity, the trade-off is also more amenable to measurement than the plethora of underlying finer-scale mechanisms. Although the differential equation model reproduced the qualitative results of the individual-based model, the predicted abundance distribution is not log-normal (except for very special choices of the form of the trade-off). An explicit account of space, as in the individual-based model, seems to be required to produce the log-normal form of the abundance distribution at equilibrium. Neither geneflow nor mutation are essential processes in the generation or maintenance of the log-normal form, although they are likely to modify the associated parameters (Box 1).

We have shown that significant diversity in traits can be sustained on small spatial domains, and that this diversity possesses the observed forms of community-scale patterns. This suggests that progress can be made using relatively small systems which are amenable to experimentation, and replacing species with individuals as the fundamental ecological accounting unit. □

Received 12 October 2000; accepted 18 January 2001.

1. Sole, R. V., Manrubia, S. C., Benton, M., Kauffman, S. & Bak, P. Criticality and scaling in evolutionary ecology. *Trends Ecol. Evol.* **14**, 156–160 (1999).
2. West, G. B., Brown, J. H. & Enquist, B. J. A general model for the structure and allometry of plant vascular systems. *Nature* **400**, 664–667 (1999).
3. MacArthur, R. M. On the relative abundance of species. *Am. Nat.* **94**, 25–36 (1960).
4. Sugihara, G. Minimal community structure: an explanation of species abundance patterns. *Am. Nat.* **116**, 770–787 (1980).
5. Ugland, K. I. & Gray, J. S. Lognormal distributions and the concept of community equilibrium. *Oikos* **39**, 171–178 (1982).
6. Tilman, D. & Kareiva, P. *Spatial Ecology* (Princeton Univ. Press, Princeton, 1997).
7. Giplin, M. & Hanski, I. *Metapopulation Dynamics: Empirical and Theoretical Investigations* (Academic, London, 1991).
8. Putman, R. J. *Community Ecology* (Chapman and Hall, London, 1994).
9. Hubbell, S. P. A unified theory of biogeography and relative species abundance and its application to tropical rain forests and coral reefs. *Coral Reefs* **16** (suppl.), S9–S21 (1997).
10. Huston, M. A. *Biological Diversity: The Coexistence of Species on Changing Landscapes* (Cambridge Univ. Press, Cambridge, 1994).
11. Durrett, R. & Levin, S. A. The importance of being discrete (and spatial). *Theor. Popul. Biol.* **46**, 363–394 (1994).
12. Winkler, E., Fischer, M. & Schmid, B. Modelling the competitiveness of clonal plants by complementary analytical and simulation approaches. *Oikos* **85**, 217–233 (1999).
13. Pacala, S. W. Neighbouring models of plant population dynamics. 2. Multi-species models of annuals. *Theor. Popul. Biol.* **29**, 262–292 (1986).
14. Crawley, M. J. & May, R. M. Population dynamics and plant community structure: competition between annuals and perennials. *J. Theor. Biol.* **125**, 475–489 (1987).
15. Rosenzweig, M. L. *Species Diversity in Space and Time* (Cambridge Univ. Press, Cambridge, 1995).
16. Legendre, L. & Legendre, P. *Numerical Ecology* (Elsevier, Amsterdam, 1983).
17. Lorequ, M. Species abundance patterns and the structure of ground-beetle communities. *Ann. Zool. Fennici* **28**, 49–56 (1992).
18. Pearson, T. H., Gray, J. S. & Johannessen, P. J. Objective selection of sensitive species indicative of pollution-induced change in benthic communities. 2. Data analyses. *Mar. Ecol. Prog. Ser.* **12**, 237–255 (1983).

**Acknowledgements**

We thank U. Bausenwein and P. Millard for supplying the *Rumex acetosa* data used in the model. This work was partly funded by SERAD.

Correspondence and requests for materials should be addressed to J.W.C. (e-mail: j.crawford@tay.ac.uk).

**Sustainability of three apple production systems**

John P. Reganold\*, Jerry D. Glover\*, Preston K. Andrews† & Herbert R. Hinman‡

\* Department of Crop and Soil Sciences, Washington State University, Pullman, Washington 99164, USA

† Department of Horticulture and Landscape Architecture, Washington State University, Pullman, Washington 99164, USA

‡ Department of Agricultural Economics, Washington State University, Pullman, Washington 99164, USA

Escalating production costs, heavy reliance on non-renewable resources, reduced biodiversity, water contamination, chemical residues in food, soil degradation and health risks to farm workers handling pesticides all bring into question the sustainability of conventional farming systems<sup>1–4</sup>. It has been claimed<sup>5,6</sup>, however, that organic farming systems are less efficient, pose greater health risks and produce half the yields of conventional farming systems. Nevertheless, organic farming became one of the fastest growing segments of US and European agriculture during the 1990s<sup>7,8</sup>. Integrated farming, using a combination of organic and conventional techniques, has been successfully adopted on a wide scale in Europe<sup>9</sup>. Here we report the sustainability of organic, conventional and integrated apple production systems in Washington State from 1994 to 1999. All three systems gave similar apple yields. The organic and integrated systems had higher soil quality and potentially lower negative environmental impact than the conventional system. When compared with the conventional and integrated systems, the organic system produced sweeter and less tart apples, higher profitability and greater energy efficiency. Our data indicate that the organic system ranked first in environmental and economic sustainability, the integrated system second and the conventional system last.

Organic management practices combine traditional conservation-minded farming methods with modern farming technologies but exclude such conventional inputs as synthetic pesticides and fertilizers, instead putting the emphasis on building up the soil with compost additions and animal and green manures, controlling pests naturally, rotating crops and diversifying crops and livestock<sup>10</sup>. Organic farming systems in the US range from strict closed-cycle systems that go beyond organic certification guidelines by limiting, as much as possible, external inputs to more standard systems that simply follow organic certification guidelines. Integrated farming systems reduce the use of chemicals by integrating organic and conventional production methods.

Just because a system is organic or integrated does not ensure its sustainability; nor does sustainability, an inherently complex

**Table 1 Soil quality ratings of three apple production systems**

Soil quality functions	Year	Organic	Conventional	Integrated
Accommodate water entry	1998	0.21a	0.16b	0.23a
	1999	0.21a	0.16b	0.20ab
Facilitate water movement and availability	1998	0.21a	0.21a	0.24b
	1999	0.19a	0.18a	0.20a
Resist surface structure degradation	1998	0.23ab	0.19a	0.24b
	1999	0.21a	0.15b	0.21a
Sustain fruit quality and productivity	1998	0.24a	0.23ab	0.21b
	1999	0.22a	0.21a	0.21a
Total soil quality rating	1998	0.88a	0.78b	0.92a
	1999	0.83a	0.70b	0.81a

Soil quality functions (each with a maximum value of 0.25) were assigned values on the basis of soil properties analysed and then added to determine soil quality ratings for each system. A total soil quality rating of 1.0 represents soil conditions optimal for both fruit production and environmental quality. Differences between values in a year followed by different letters are significant at the 0.05 level (least significant difference).